



OPEN Statistical analyses of precious metal contents in waste incineration bottom ashes

Monika Chuchro^{1✉}, Radosław Jędrusiak² & Barbara Bielowicz³

The recovery of precious metals from incinerator bottom ash (IBA) is a way of moving towards a circular economy. The paper presents a detailed analysis of the concentration of precious metals in IBA. The average values of precious metals in the samples analyzed are: Ag—6973 ppb, Au—313.90 ppb, Pd—41.26 ppb, Pt—13.81 ppb—all of these values being many times higher than the values of these elements in the Earth's crust. The time series of the precious metals in the IBA were analyzed to assess the trend, seasonality, and outliers and to detect differences between the designated seasons of the year. Data analysis was performed following the CRISP-DM methodology using statistical and data mining methods. The analyzes confirmed a higher Ag concentration than in comparable European waste incinerator plants. The Au concentration was comparable to those reported in other incinerators, while the values were lower for Pt and Pd. The time series of precious metals shows no trend and seasonality, but numerous outliers. Due to the stationarity of precious metals, recovery can be expected to be constant, and the presence of numerous outliers can increase the potential return on investment.

Keywords Incinerator bottom ash, Precious metals, CRISP-DM, Municipal waste, Time series analysis, Precious metals recovery

Municipal waste management is one of the major problems in developing economies. Between 7 and 10 billion tons of waste are produced annually worldwide, including about 2 billion tons of municipal waste¹. The amount of municipal waste generated in the European Union in 2021 was 236 million tons². This is 12% of the municipal waste generated worldwide. As a result of the perceived problem, the European Union authorities have obliged member states to radically change their approach to waste by introducing a five-step waste hierarchy. In addition to the main priorities in the hierarchy, which are waste prevention, analysis of the impact of various waste management methods on the natural environment, and preparation for reuse, there is increasing pressure on waste recycling^{3–6}. As a result of the implemented regulations, member countries are obliged to increase the share of waste recycling to at least 65% by 2035⁷. The current average recycling rate in European countries is 43% and its theoretical upper limit is estimated at 80%⁸. Therefore, despite many controversies, waste energy recovery (thermal processing of municipal waste) will play an important role in the circular economy system⁹. Undoubtedly, the main benefits of incinerating non-recyclable waste are both the weight reduction of approximately 75%¹⁰ and energy recovery in the form of electricity and heat in the cogeneration process¹¹. Increasing attention is also being paid to the recyclability of incineration residues. Incineration bottom ashes^{12,13} account for around 25% of incineration waste. The most common recovery methods include the recovery of ferrous and non-ferrous metals commonly found in bottom ash^{13–15}. The average share in bottom ash is 5–15% in the case of ferrous metals and 1.0–5.0% for non-ferrous metals. The fine fraction < 4 mm, although it constitutes a negligible share of the total metals found in the bottom ash and amounts to only about 0.3%, could be a significant component of waste processing revenues due to the presence of heavy metal fractions, including precious metals^{16–18}, as shown in Fig. 1.

In 2013, silver at 5.30 mg/kg, gold at 0.40 mg/kg, and platinum group elements (platinum at 0.059 mg/kg) were found in the feedstock to be incinerated in Switzerland¹⁹. The transfer of these elements from incinerated waste to bottom ashes ranged from 69 to 100% and the concentration of precious metals in bottom ashes was: silver 20.1 mg/kg, gold 1.9 mg/kg, and in the platinum group: platinum 0.27 mg/kg²⁰. In 2015, the presence of precious metals was found in bottom ashes from the Italian waste incinerator plant with the following amounts:

¹Department of Geoinformatics and Applied Computer Science, Faculty of Geology, Geophysics and Environment Protection, AGH University of Krakow, Krakow, Poland. ²Krakowski Holding Komunalny S.A. w Krakowie, Krakow, Poland. ³Department of Geology of Mineral Deposits and Mining Geology, Faculty of Geology, Geophysics and Environment Protection, AGH University of Krakow, Krakow, Poland. ✉email: chuchro@agh.edu.pl

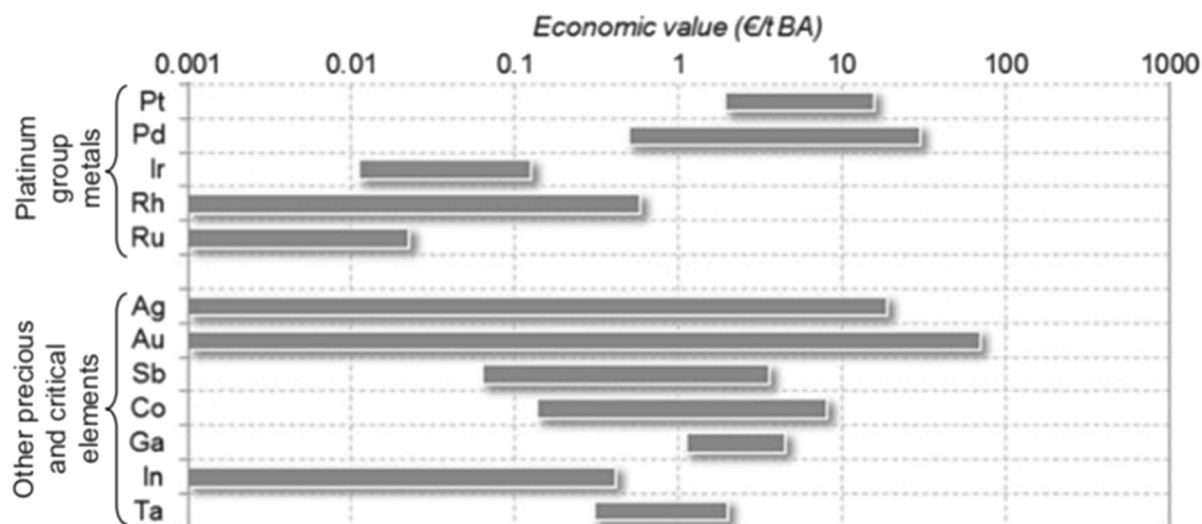


Fig. 1. Estimated total economic value of precious metals contained in bottom ashes from municipal waste incineration (based on¹⁸).

silver 5.51 mg/kg and gold 0.44 mg/kg²¹. Precious metals are present in small quantities in components of waste electrical and electronic equipment²² and their presence in bottom ashes from municipal waste incineration indicates an inefficient selective waste collection system and the lack of specialized sorting devices in mechanical–biological treatment plants. Another source of precious metals in waste is jewelry lost by people who live in the area from which municipal waste is collected. Potentially recoverable larger forms of metals (> 2 mm) occur as separate components, such as jewelry or coins, or as composites, such as gold-plated stainless steel watch bands. Significant amounts of precious metals found in bottom ashes are also present in the fine fraction (< 2 mm)—they come from silver-soldered items or gold-plated contacts²⁰. Precious metals naturally occur in the Earth's crust in the following amounts: silver 0.0075 mg/kg, gold 0.0004 mg/kg, platinum 0.0005 mg/kg, palladium 0.0015 mg/kg²³. In 2023, the European Commission updated the list of critical raw materials for the EU (the list is updated every three years). Critical raw materials are those raw materials that are of high importance to the EU economy, and, at the same time, whose supply is associated with a high risk. The assessment of critical raw materials considers the economic importance and the high risk of supply disruption. Critical Raw Materials (CRMs) are those for which the coefficient of economic importance (EI) is ≥ 2.8 and the coefficient related to the supply risk (SR) is ≥ 1.0 . As a result of the 2020 criticality assessment, platinum group metals retained their status as critical raw materials while gold and silver were not included in the list. In the case of gold, the EI value increased from 2.1 to 2.4 and the SR value increased from 0.2 to 0.4, for silver, the EI value increased between 2020 and 2023 from 4.1 to 4.6 and the SR value increased from 0.7 to 0.8²⁴. In Poland, the first modern municipal waste treatment plant was launched in 2000 in Warsaw, but most municipal waste incinerator plants started to operate in the second decade of the twenty-first century thanks to financial support from the European Union Cohesion Fund²⁵. To date, comprehensive analyses of bottom ash from municipal waste incineration from the Polish waste management system have not been published. For this reason, it was decided to conduct a detailed analysis of the content of precious metals in bottom ashes. This analysis was based on chemical data obtained from samples taken weekly in 2021. This paper is the first to analyze the concentration and variability of precious metals in bottom ashes from waste incineration.

Materials and methods

Research subject

The research concept for the analysis of the precious metal content in bottom ashes from municipal waste incineration was developed in 2020 at the Krakow Thermal Waste Treatment Plant²⁶. The Thermal Waste Treatment Plant in Krakow was commissioned in 2016; the total net cost of the project was approximately EUR 155 million net. The plant has two independent incineration lines connected to each other by the electricity generation and transmission node (extraction condensing turbine). Each line processes up to 15.5 Mg of waste per hour, and the total processing capacity of the plant is 245,000 Mg/year. The feedstock used consists of two streams of municipal waste from the city of Krakow. The first and main stream is waste with the EWC code 19 12 12, originating from the mechanical and biological treatment of municipal waste (approximately 65% share). The second waste stream, accounting for about 35%, is a non-recyclable municipal waste with the EWC code 20 03 01, collected directly from residents, as part of a separate waste collection system. The combustion technology used uses a grate furnace integrated with a natural circulation steam boiler. The bottom ash produced is directed to a slag trap equipped with a water lock, from where, after cooling, it is passed through a conveyor belt unit onto ferrous metal separators. The obtained bottom ash is then subjected to a two-week weathering process, where the moisture content is reduced from around 30% to around 12–20%. After the pre-weathering process, in the

incineration plant, bottom ash is processed in an installation where ferrous and non-ferrous metals are partially recovered and the produced metal concentrates and impurities in bottom ash with different grain sizes.

Sampling and analysis

The samples used for the research were taken from bottom ash and subjected to a preliminary two-week weathering process and a partial metal recovery process. The sampling was carried out on one day of each week, beginning in January and ending in December 2021. The samples were taken according to the requirements of PN-EN 14899 sampling of waste materials. Framework for the preparation and application of a sampling plan²⁷ and the guidelines for bottom ash sampling set out in the study “List of methods—Sampling and preparation of samples and analysis of solid residues from thermal treatment of waste and products generated during treatment”²⁸. Eight primary samples of bottom ash weighing 3.5–4.0 Mg were collected per day. Samples were taken from the end of the conveyor belt (from the falling waste stream) using a wheel loader equipped with a weighing system. The eight samples taken in this way, with a total maximum weight of 32.0 Mg, formed a composite sample, which was then directed to be reduced in size; finally, a longitudinal two-row prism was formed. There were four primary samples in each row of the pile. Reducing the sample size involved dividing the pile into two equal parts. Splitting was done by digging up the pile from the shorter side. The first pile was directed to the next stage of reduction and the second pile was rejected. In the last stage, two piles with a mass of about 8.0 Mg were obtained, and the collection from these piles was carried out along their diagonals. At this stage, approximately 300.0 kg of material was collected, which was fed to a sample divider (DP, Multiserw); as a result about 10.0 kg laboratory samples were obtained. The samples were crushed to < 2 mm (Terminator Jaw Crusher, TM Engineering LTD) and then ground (LM201, ESSA FLSmidth) to a size of < 75 µm. The analysis of the chemical composition was performed using inductively coupled plasma mass spectrometry. Laboratory samples weighing about 100 g were pre-digested in a 1:1:1 aqua regia solution (HNO₃, HCl, H₂O). The results obtained for the precious metal content expressed in ppb are presented in Annex 1. Values under detection limit (UDL) and above detection limit (ADL) are marked with a majority or minority sign, respectively. Determination of precious metal content was carried out using a Perkin Elmer ELAN 9000 mass spectrometer. Quality control was conducted using multi-element custom-certified reference materials STD BVGEO01 and STDORAS262. Analysis of a blank sample and a control duplicate analysis of one of the samples was performed to assess the repeatability of the results.

Data analysis

The assessment of the potential recovery of precious metals from bottom ash from municipal waste incineration at the Thermal Waste Treatment Plant in Kraków was carried out in accordance with the cross-industry standard Process for Data Mining (CRISP-DM) methodology, which is one of the most widely used methodologies for data analysis^{29–32}. This methodology defines six key phases that enable the execution, evaluation, and implementation of models supporting business decision-making. The advantage of the CRISP-DM methodology is the possibility of returning to earlier phases in case of unsatisfactory results^{29,31}.

The first CRISP-DM Phase—*Business Understanding*—task is aimed at defining the objectives of the planned analysis. It can be considered that if the elemental content of IBA does not change over time, i.e. is stationary, and occurs in average quantities like those of other waste incinerators with similar processing capabilities where precious metal recovery has been implemented, then its recovery can be cost-effective. Furthermore, if only single precious metals are present in high values, it may turn out that potentially unprofitable precious metals, will also be profitable if the recovery is carried out completely, i.e. by choosing the right recovery technique. An additional argument for the implementation of the precious metal recovery project from bottom ashes is the observation of the occurrence of outliers and extremely high values.

The *Data Understanding* phase involved performing a descriptive analysis of the data³³. The data analyzed constituted a data frame containing a time series of four precious metals: silver, gold, palladium, and platinum. A single time series contained 52 observations measured in week intervals. The time series for silver and palladium contained “censored” observations, which means that part of the obtained results was below or above the limit of quantification of the analytical method used. In the case of silver, there was one observation above the detection range of the measuring device, the so-called ADL, while the time series for palladium contained 14 observations below the detection range of the measuring device, the so-called UDL.

The next phase—*Data Preparation*—involved preparing data to assess the possibility of extracting precious metals from bottom ash after municipal waste incineration. Proper data preparation is crucial to obtain optimal results of the analysis. Censored data should never be deleted from the dataset to avoid a strong bias in estimating descriptive statistics and model results. Censored observations should be replaced. In the imputation method, a value is assigned to each censored observation. In datasets with more than 15%, and less than 50% of censored observations it is advisable to use extrapolation methods, Robust Regression on Order Statistics (ROS), Kaplan–Meier method, Cohen’s method, Weibull regression, or Maximum likelihood estimation (MLE)³⁴.

At this stage, the UDLs for palladium were replaced by values calculated using the Robust Regression on Order Statistics (ROS) method^{35,36}. It is one of the recommended methods to replace censored values for environmental data for small datasets³⁷.

After replacing the censored value with the ROS method, basic descriptive statistics were performed. In addition, bar charts, autocorrelation function plots, seasonality plots, and ANOVA analysis were performed^{38,39}. In this phase, stationary data analysis—the Augmented Dickey–Fuller test—was also performed⁴⁰.

The next phase—*Modelling*—has been modified for the requirements of the project. In this phase, the focus was on assessing the relationship between precious metals. Therefore, the Pearson and Spearman’s rank correlation matrices^{41,42} were used. Pearson’s correlation assesses linear relationships, while Spearman’s correlation assesses monotonic relationships. The use of both Pearson’s linear correlation and Spearman’s ranks allows assessing the

correlation power, direction, and shape of the correlation⁴¹. To supplement the correlation matrices, scatter plots were made for statistically significant correlations.

In this phase detection of the high and very high content of precious metals in individual samples was performed. Moreover, attempts were made to find out whether the high values of one precious metal were related to the high values of another. An analysis of the occurrence of outliers and extreme values was carried out using the Rosner test⁴³.

The last step was to compare the mean values using a one-sample t-test⁴⁴. The average values of the IBA precious metals content were compared with the given average values for the Hinwil incineration plant⁴⁵, in Northern Italy²¹ and their average content in the Earth's crust⁴⁶.

The *Evaluation*—phase is presented in the Discussion and Conclusions sections. At this stage of the project, the analyzes performed were interpreted and conclusions regarding the recovery of precious metals from IBA were presented.

The *Deployment*—phase of the CRISP-DM methodology involves implementing a ready-made solution—in this case, the beginning of the recovery of precious metals. This phase was omitted.

Theoretical issues of data analysis

Robust Regression on Order Statistics (ROS) is a semi-parametric statistical method that computes a regression line to estimate values for censored data. ROS assumes that the underlying population is normally or lognormally distributed. Additionally, in the data, there should be at least three detected values and a detection frequency greater than 50%. The ROS method is based on a simple linear regression model that uses ordered detected values and distributional quantiles to estimate the concentration of the censored values. ROS imputes the censored data using the estimated least-squares linear model parameters and estimates the overall sample mean and sample deviation.

Robust regression on order statistics can be presented as follows³⁵:

for $n = n_0 + n_1$ independent normally distributed data, with mean μ and variance σ^2 ,
 n_0 is the observations are non-detects, n_1 is the observations are larger than the detection limit.

$$y_i = \mu + \sigma \Phi^{-1}(P_i) \quad (1)$$

where: $P_i = P(Y_i \leq y_i)$ and $\Phi^{-1}(\cdot)$ denotes the inverse cdf of a $N(0,1)$ distribution.

The procedure replaces probabilities with adjusted ranks; the regression equation becomes:

$$y_i = \hat{\mu} + \hat{\sigma} \Phi^{-1} \left(\frac{i - 3/8}{n + 1/4} \right) + \varepsilon_i \quad (2)$$

where: $i = n_0 + 1, n_0 + 2, \dots, n_0 + n_1$, $\hat{\mu}$, $\hat{\sigma}$ is the least squares estimates of μ , $\Phi^{-1} \left(\frac{i - 3/8}{n + 1/4} \right)$ is the normal score calculated using Altman's formula, ε_i is the residual errors.

One-way analysis of variance (ANOVA) is one of the most frequently used statistical methods to determine the significance of differences between data subsets. Analysis of variance is used when there are at least three mutually independent groups with normal distribution and similar variance. ANOVA uses the F -for statistical significance. The F-test compares the variance in each group mean from the overall group variance. If the variance within the group is smaller than the variance between groups, the F-test obtains a higher F value, and thus a higher likelihood that the observed difference is significant. The null hypothesis is that there is no statistically significant difference between group means. The alternative hypothesis is that there are at least two groups that are statistically significantly different from each other^{39,44}.

A *one-sample t-test* is a statistical test used to determine whether an unknown population mean is different from a specific value⁴⁴. This test should be performed for large samples (more than 30 observations). The t-test is highly sensitive to non-detects⁴⁷.

The one-sample t-test can be presented as⁴⁴:

$$t = \sqrt{n} \frac{\bar{x} - \mu}{s} \quad (3)$$

where the test has the t -distribution with $n - 1$ degrees of freedom for n ($n \geq 30$), $p = 0.05$, and: \bar{x} is the mean value in sample, μ is the value of comparison, s is the standard deviation in the sample.

The null hypothesis (H_0) is that the true difference between the sample mean, and the comparison value is zero.

The alternative hypothesis (H_a) is that the true difference is different from zero.

There are several methods to test the stationarity of time series. The initial information is obtained thanks to the *Autocorrelation function* (ACF). The ACF helps to recognize the stationarity, trend, and seasonality of data. The autocorrelation function for lag k is Pearson's linear correlation coefficient between a given time series and the same time series separated by k intervals³⁸. The ACF function is well discussed in the literature^{38,48,49}.

The *Augmented Dickey-Fuller test* (ADF) is a unit root test for stationarity that can be used with serial correlation. The null hypothesis is there is a unit root in the first-order AR model, which implies that the data series is not stationary. The alternative hypothesis is stationarity or trend stationarity and depends on the test version⁵⁰.

ADF statistics can be presented as:

$$\Delta y_t = \mu + \gamma y_{t-1} + \sum_{i=1}^P \alpha_i \Delta y_{t-i} + \varepsilon_t \quad (4)$$

$$ADF = \frac{\hat{\gamma}}{SE(\hat{\gamma})} \quad (5)$$

The maximum lag value is expressed as follows⁵⁰:

$$nlag = \left(\frac{4 \bullet n}{100} \right)^{\frac{2}{9}} \quad (6)$$

where: μ is the mean value, γy_{t-1} is the lagged values of the dependent variable, ε_t is the white noise, n is the number of observations.

The computed ADF value can be compared to the relevant critical values for the Dickey–Fuller test. This test is asymmetrical, so concerned with negative values of test statistics. If the calculated statistical test is more negative than the critical value, then the null hypothesis is rejected, and no unit root is present⁵⁰.

The *Rosner test* detects up to 10 outliers among the selected data values. The test can detect outliers that are much smaller or much larger than the rest of the data and avoids the masking problem (when two outliers have similar values, one of them could go undetected). Data are ordered in ascending order. In the next step the k number of suspected outliers is specified. Then a series of statistics excluding the largest and smallest observation from the data is calculated. The test equation is as follows:

$$R_{i+1} = \frac{|x^{(i)} - \bar{x}^{(i)}|}{s^{(i)}} \quad (7)$$

Critical values for R_{i+1} are denoted λ_{i+1} and can be presented as:

$$\lambda_{i+1} = \frac{t_{p,n-i-2}(n-i-1)}{\sqrt{(n-i-2 + t_{p,n-i-2}(n-i))}} \quad (8)$$

where $t_{p,\nu}$ denotes the p 'th quantile of Student's t -distribution with ν degrees of freedom, and can be presented as:

$$p = 1 - \frac{\alpha/2}{n-1} \quad (9)$$

where: $\bar{x}^{(i)}$ is the sample mean, $x^{(i)}$ is the observation in data subset that is the furthest from $\bar{x}^{(i)}$, $s^{(i)}$ is the data standard deviation after removing the i most extreme observations, α is the Type I error level (0.05, as long as $n \geq 25$).

Rosner's test is based on k statistics R_1, R_2, \dots, R_k which represent the extreme studentized deviates computed from successively reduced samples of size $n, n-1, \dots, n-k+1$. A series of hypothesis tests is performed after all test statistics $R_1 \dots R_k$ are computed. Null hypothesis: there are no outliers in the data. Alternative hypothesis: there are k outliers in the data. The first test assumed that there were k outliers in the data, by comparing R_k to the critical value λ_k for a specified significance level α . If $R_k > \lambda_k$, then the test is significant and the null hypothesis is rejected, and in data k the most extreme values are outliers^{43,51}.

Software used

During the data analysis, the R 4.2.3 package was used (Shortstop Beagle released 2023-03-15), together with the integrated RStudio 2023.03.1 (Cherry Blossom released 2023-05-09). The following packages were used: aTSA v3.1.2, corrplot v0.92, dplyr v1.0.10, e1071 v1.7-11, EnvStats v2.7.0, forecast v0.5.2, ggplot2 v3.3.6, NADA v1.6-1.1, stats 4.4.0, tidyr v1.2.1, and tseries v0.10-52. The calculations were performed on a computer with the Windows 11 Pro 64-bit operating system with an i7-10710 processor with 1.10 GHz and 16 GB RAM.

Profitability analysis

The following average precious metal prices from the London Metal Exchange for June 2023 were used to assess cost-effectiveness: 0.797 EUR/g (silver), 64.916 EUR/g (gold), 47.021 EUR/g (palladium), and 34.399 EUR/g (platinum)⁵². The estimated capital expenditure for the construction of a state-of-the-art facility for the recovery of metals from bottom ash was based on the capital expenditure incurred for the construction of the Afatek A/S in Denmark with a capacity of 180,000 Mg per year. The amount of capital expenditure was then increased by the producer price index, whose value between 2016 and 2023 was 1,551⁵³; the capital expenditure associated with the construction of a 50,000 Mg/year plant was then estimated on this basis. Investment expenditures in 2023 were estimated at EUR 3.447 million. The recovery efficiency was determined based on data from the Hinwil plant at the level of: 57.4% for silver, 28.8% for gold, and 30.0% for platinum and palladium⁵⁴. Electricity consumption was determined at 8.28 kWh / Mg IBA, based on data collected by Bruno, M. et al. 2021⁵⁵, and the cost of 1 MWh of electricity was assumed at 129.1 EUR⁵⁶. Maintenance costs were assumed for years 1–2 at 1.25% CAPEX and for years 3–20 at 2.5% CAPEX. The costs of laboratory tests were assumed at EUR 25,000 per year, and the costs of salaries for employees operating the installation were assumed at EUR 80,000 per year.

Subsequently, the obtained data were used to determine the internal rate of return. The IRR is used to estimate the return on potential investments⁵⁷. Then, based on the internal rate of return obtained, the payback time was calculated. The internal rate of return was calculated from the formula:

$$IRR = \sum_{t=1}^n \frac{CF_t}{(1+d)^t} - I_0[EUR] \quad (10)$$

where: CF_t is the cash flow, I_0 is the investment cost, d is the discount rate (4.4%), t is the plant lifetime (20 years).

The determination of discount rate was carried out in the range from 0 to 10%. The cutoff value was between 4 and 5%. In the first case, the NPV was positive and close to zero, while for a rate equal to 5% the NPV was negative, but still close to zero. The exact discount rate was determined using the following formula:

$$d \approx i_1 + \frac{NPV_1 \times (i_2 - i_1)}{NPV_1 + NPV_2} [\%] \quad (11)$$

where: i_1 is the discount rate for NPV_1 [%], i_2 is the discount rate for NPV_2 [%], NPV_1 is the positive NPV value for 4% discount rate [EUR], NPV_2 is the negative NPV value for 5% discount rate [EUR].

Results

In the first step, preprocessing was performed, which included replacing the UDL values for palladium and the ADL values for silver. In the palladium time series, UDL values occurred 14 times and were 27% of the total number of observations. The silver data had 1 ADL observation. The UDL and ADL observations were replaced according to the recommendations of the US Environmental Protection Agency and described in detail in publications:^{35–37,58}. The actual values and replacements are shown in Fig. 2.

The silver content in bottom ash samples is the highest among all analyzed precious metals. The average silver content is 6,973 ppb. The significant difference between the mean value and the median indicates the right-sided skewness of the data distribution, and thus the occurrence of observations with high and very high silver content, which is also confirmed by the skewness coefficient of 4.5. The distribution is asymmetric, tapered for values below 20,000 ppb, with outliers on the right (see Table 1). The maximum value for silver is not known, due to the presence of an ADL value, which was estimated to be 100,980 ppb using the random value from the data distribution (Table 1).

The gold content in the bottom ash samples is significantly lower than the silver content. The mean value was 313.9 ppb and was almost 7 times higher than the median value. The standard deviation of 1,172 indicates a large dispersion of observations around the mean value, as can be seen in Table 1. The skewness of the data was high. In the case of gold, there were no censored observations; despite this, the distributions for gold and silver have a similar shape.

The palladium in the analyzed waste samples was below the level of quantification (UDL) in 14 observations; therefore, the minimum value is the value obtained with ROS. Due to the use of ROS, there is no distortion in

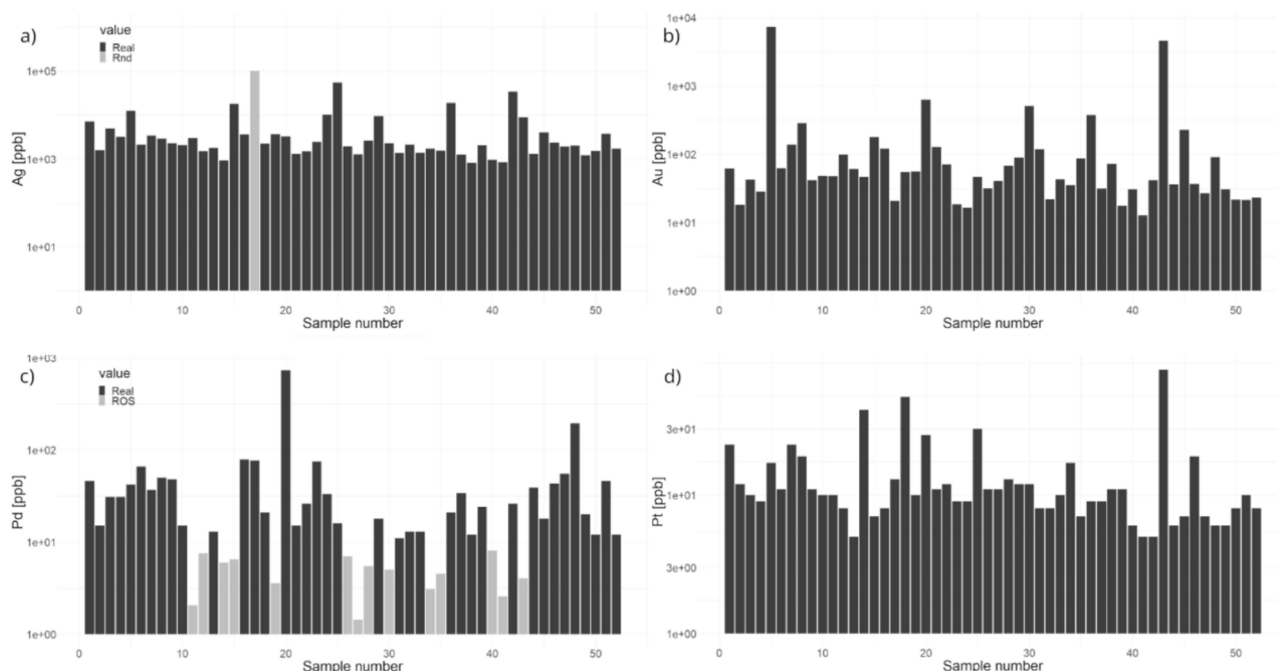


Fig. 2. The content of precious metals in individual samples; (a) silver, (b) gold, (c) palladium, (d) platinum. Logarithmic scale; values replacement marked with grey.

Compound	Minimum	Mean	Median	Maximum	Standard deviation	Skewness	Estimated annual flow (kg)	Hinwil* (Morf et al. 2013)	Northern Italy* (Funari et al. 2015)	Other studies* (Astrup et al. 2016)	Earth's crust content* (Haynes 1942)	IBA Enrichment factors* (Buat-Menard & Chesselet 1979)
Ag	817.0	6,973.0	2,154.0	100,980.0	16,033.8	4.5	348.7	5,300	5,510	< 290 – 36,900	75	29
Au	12.7	313.9	47.1	7,281.6	1,171.9	5.0	15.7	400	410	< 110 – 2,200	4	12
Pd	1.4	41.3	18.0	731.0	102.4	5.9	2.1	NA	NA	800–1,000	15	1
Pt	5.0	13.8	10.0	80.0	12.8	3.4	0.7	59	NA	74 – 530	5	2

Table 1. Descriptive statistics [ppb]. *References: [18](#),[21](#),[46](#),[59–61](#).

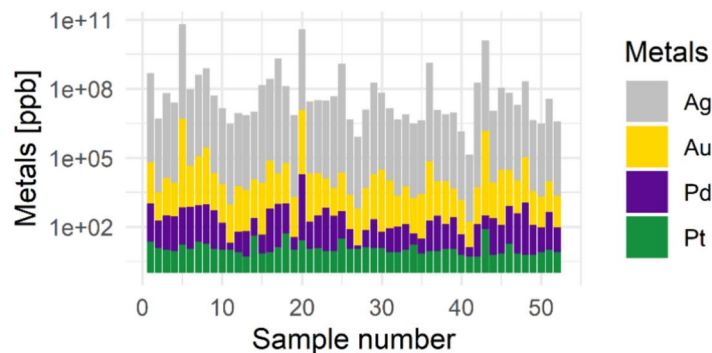


Fig. 3. The content of precious metals in individual samples.

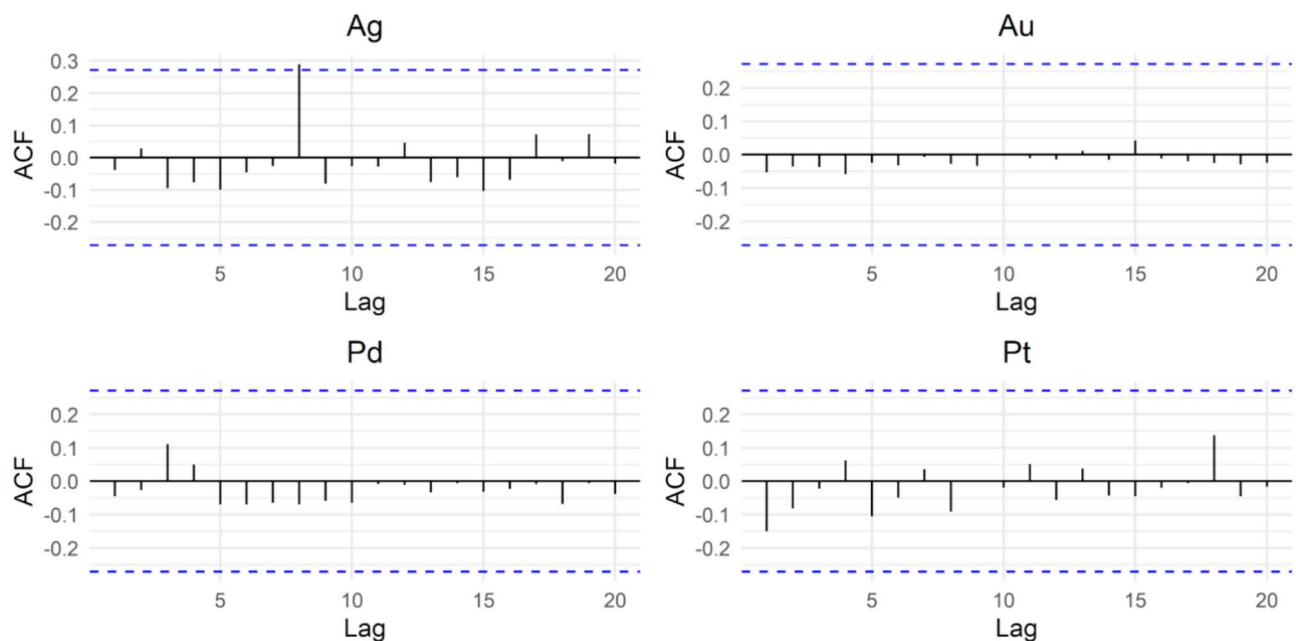


Fig. 4. Autocorrelation function plots (black line) with critical values at the 5% significance level (blue dashed line); (a) silver, (b) gold, (c) palladium, (d) platinum.

the most calculated descriptive statistics and distribution. The average palladium content was 41.3 ppb and was more than 2 times higher than the median. The maximum value was 731 ppb and was more than 17 times higher than the average value (see Table 1). The distribution for palladium also shows high skewness and the occurrence of outliers. These data show the highest skewness among the precious metals (Table 1).

The last precious metal analyzed was platinum. It was present in the waste in the smallest amounts among the analyzed metals. The average platinum content was 13.8 ppb and was less than 40% higher than the median. The standard deviation and the skewness coefficient indicate a smaller dispersion of data around the mean value and the lowest skewness among the analyzed data. In the platinum time series, observations with high and very high values are much less frequent compared to the other precious metals (Table 1). The platinum distribution is more symmetric than in other precious metals. Lower data skewness and variance make the distribution more like a typical Gaussian distribution (Table 1).

By analyzing the sum of precious metals, one can observe small dependencies between their occurrence, which is presented in Fig. 3. For observations 5, 20, 36, and 43, high contents of platinum, gold, and silver contents are seen (Supplementary 1, Fig. 3). Observations 13, 26, and 41 are characterized by a lower content of platinum, palladium, and gold but an average silver content (Annex 1, Fig. 3). There is no clear seasonality in the graph (Fig. 3); neighboring observations differ significantly in the sum of metal content. From 25 to 41 observations, there seems to be a decrease in the sum of the analyzed metal contents in the samples (summer and early fall). Low palladium content is observed more commonly during this period.

By analyzing the autocorrelation function plots (Fig. 4) and the results of the Augmented Dickey-Fuller test statistics, it can be assumed that the data can be considered stationary. In the ADF test statistics, the highest value was -2.92 (Pd), and the lowest was -3.91 (Ag) for lags equal to 3, and all computed statistics were statistically

significant. The autocorrelation function plots show that there are no statistically significant correlations for the lags for gold, palladium, and platinum. Such autocorrelation function plots are characteristic of time series without trend and seasonality. Additionally, no monthly or quarterly seasonality was observed on the autocorrelation plot, which would be visible on the ACF plot as statistically significant declines in correlations repeated at regular intervals (Fig. 4). In silver, ACF shows lag 8 exceed slightly the statistical significance level. This is probably a random value, since it does not repeat for higher lags (for example, lag 16). Despite the lag 8, silver can also be considered as time series without trend seasonality.

Graphs of the autocorrelation functions did not show the occurrence of a trend or seasonality for lags up to 20 (Fig. 4). However, it was decided to use box-and-whisker plots for seasonal data (Fig. 5) since the amount and morphology of municipal waste generated by the inhabitants of Krakow and therefore IBA precious metal content may be characterized by seasonality. The data were divided into 4 seasons, according to the metrological division for the northern hemisphere, which is used to compare periods of the same length and calculate statistics. According to this division: spring (1.03–31.05), summer (1.06–31.08), autumn (1.09–30.11), and winter (1.12–28.02).

The box-and-whisker plot for silver indicates the existence of a difference in the average value for silver and the asymmetry of the distribution for winter, compared to the other seasons. In addition, there is a lower variability of the data for summer and a higher variability for autumn, which is visible in Fig. 5.

In the case of gold, differences in the average level of the phenomenon for each of the seasons can be observed (Fig. 5). In spring, the median value was the highest, while in autumn this value was the lowest. The variability of the most typical values was similar for each of the seasons (Fig. 5). A characteristic feature is the location of the median within the interquartile range for spring, summer, and autumn, indicating the asymmetry of the distribution.

Palladium shows quite significant differences in average values between seasons. The lowest median values were observed for the summer period, just as for silver. Similarly to silver, the highest median values were observed in winter. The variability of the most typical data is similar for 3 seasons: spring, summer, and autumn. For winter, the variability is lower, and, in addition, the median value indicates a high skewness for this season. Box-and-whisker plots for palladium, unlike those for other precious metals, indicate the presence of only one outlier (Fig. 5).

As like silver and palladium, platinum the highest average value was observed in winter (Fig. 5). The lowest median value was observed, together with the highest value of the interquartile range, for autumn. Except for spring, the data show a distribution asymmetry (Fig. 5).

The comparison of the differences in the average level of the phenomenon is carried out using a one-way analysis of variance (ANOVA).

Despite the apparent differences in the seasonality graphs (Fig. 5), the one-way analysis of variance did not show any of the groups (seasons) to be significantly different from the others, as can be seen from the value of the F statistic equals respectively: 0.46, 0.6, 0.81, 0.27 along with its statistical significance: 0.71, 0.61, 0.49, 0.85 for silver, gold, palladium and platinum. The difference in the average level of the phenomenon for individual groups, considering the value of their variance, is too low. It cannot be stated that for any of the precious metal, there was a statistically significant difference for any of the seasons.

Two correlation measures were used in the analysis: Pearson's linear correlation coefficient and Spearman's rank correlation. The results are presented in the form of correlation charts presented in Fig. 6a, b. The use of

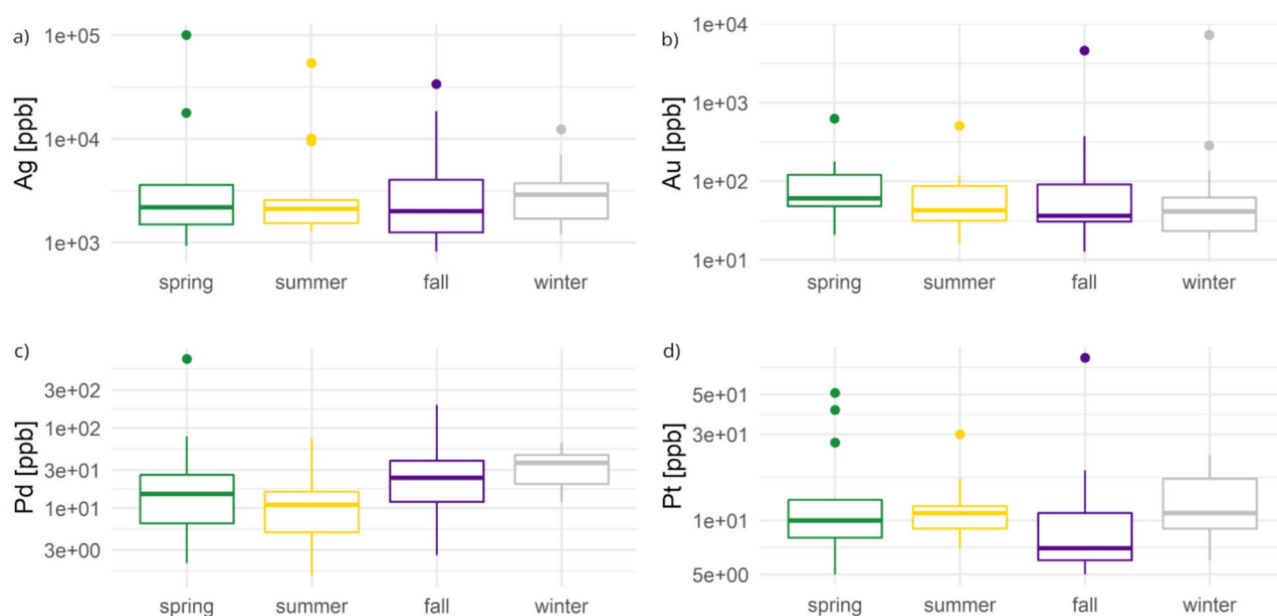


Fig. 5. Quarterly seasonality chart; (a) silver, (b) gold, (c) palladium, (d) platinum.

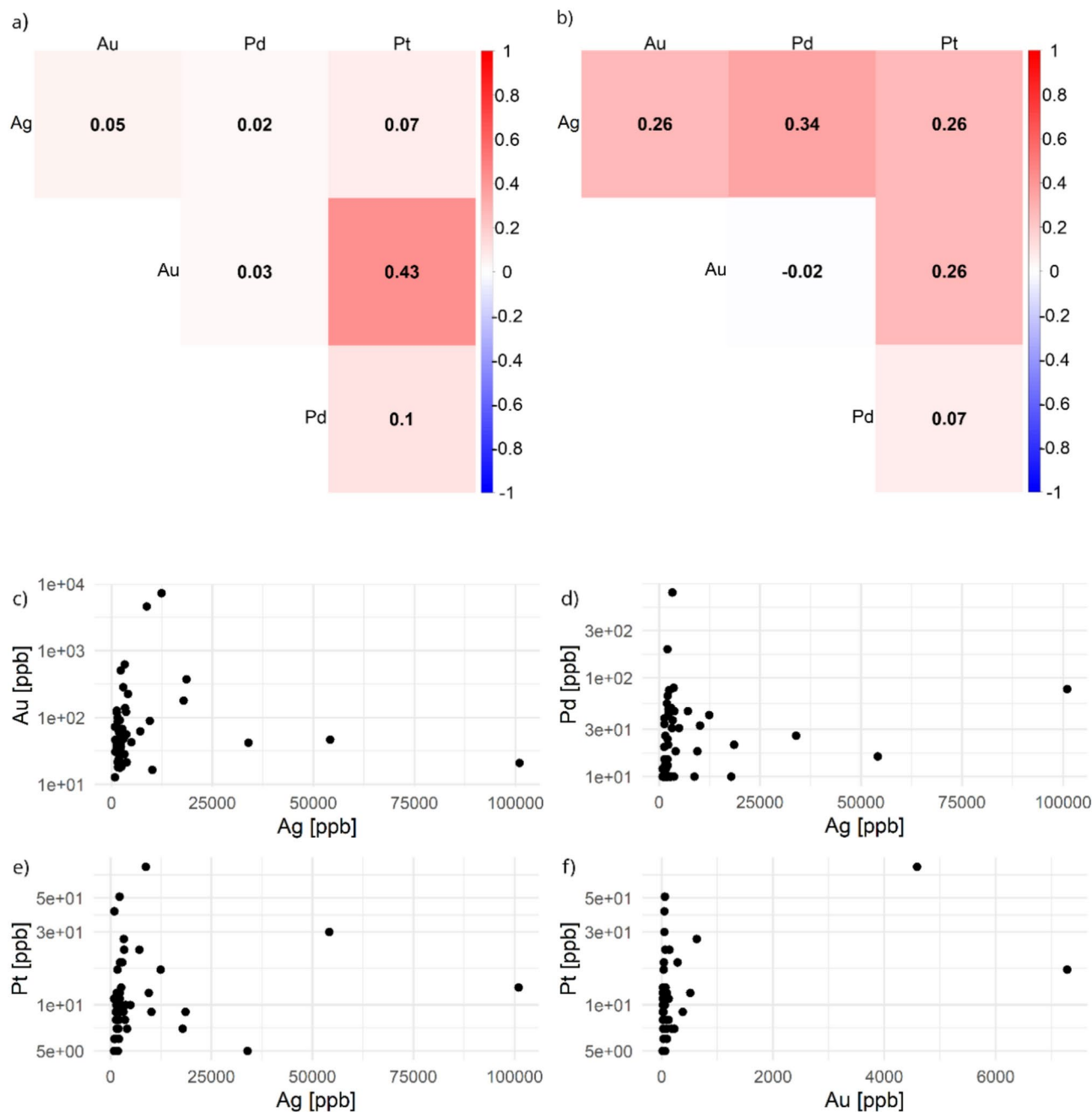


Fig. 6. Correlation charts; (a) Pearson's correlation coefficients matrix; (b) Spearman's rank correlations coefficient matrix (c) silver-gold, (d) silver-palladium, (e) silver-platinum, (f) gold-platinum.

both linear and non-parametric correlation allows us to determine the correlation power and its type. When comparing both correlation matrices, silver shows non-linear correlation relationships. Higher correlation values were observed for the Spearman rank correlation matrix for correlation with gold, the difference in correlation coefficient was 0.23 (see Fig. 6b). The correlation between silver and gold can be considered as a weak non-linear, positive, statistically significant correlation. In the case of other elements, the correlation with silver is also non-linear. The difference between the correlations for the silver-palladium relationship is 0.32 and this is the highest observed difference between the correlations. The difference in the correlation values for the silver-platinum relationship is 0.19, which is visible in Fig. 6.

Gold's correlation relationships are changeable. The correlation with silver is non-linear. The correlation between gold and platinum is linear and its strength can be considered as a positive average (0.43); the relationship is statistically significant. There is no correlation relationship between gold and palladium (Fig. 6).

The correlation relationship between platinum and palladium is non-linear and can be defined as a weak positive correlation of 0.26, which is statistically significant (Fig. 6b).

Furthermore, statistically significant correlation relationships are shown in the scatter plots (Fig. 6c–f) to fully visualize the relationship between the variables. The asymmetry of the distribution of points, related to the high variability of the data and the occurrence of potential outliers, is visible in the left part of the diagrams. Despite the flattening of the graphs for the relationship with silver, their non-linearity is visible (Fig. 6c–e). The relationship between gold and platinum seems to be of the most linear nature, which is confirmed by the value of Pearson's linear correlation coefficient (see Fig. 6a, f).

The next step of the project was to evaluate the occurrence of outliers visible in the parts of the visualizations presented above (Figs. 2, 3, 5, and 6). Rosner's test, which detected up to 10 outliers in the dataset, was performed. The results indicate the appearance of outliers for each of the analyzed precious metals. The highest number of outliers detected using Rosner's test was observed for silver. Observations with a value equal to or greater than 7.084 ppb can be considered outliers; they represent 20% of the total data (10 observations). In the case of gold, numerous outliers were also observed. Outliers were those for which the value was 179.10 ppb or more; these observations constituted 16% of the total data (8 observations). In the case of palladium, only two outliers were observed, amounting to a minimum of 195 ppb. In the case of platinum, 7 outliers were detected. The cut-off value for outliers was 23 ppb, outliers constituted 14% of the total data set.

The Hinwil incineration plant¹⁹ analyzed the elemental content of municipal waste incineration bottom ash, including silver, gold, and platinum. The average silver content of the discussed samples was 5,300 ppb with a standard deviation of 720 ppb. For gold, the average content was 400 ppb with a standard deviation of 20 ppb, and for platinum, these values were 59 ppb and 2.2 ppb, respectively (Table 1). In the case of Northern Italy, the following precious metal elements were analyzed: silver and gold. The average silver and gold contents in both incinerators were similar. In the Krakow incineration plant, the average value of silver is higher, while the value of other precious metals is lower (see Table 1).

Higher average and standard deviation values for silver in the IBA samples analyzed in this work can be observed. In the case of other precious metals, the average values are lower than in Hinwil and show higher standard deviation values (Table 1). Comparative analysis with the Northern Italy installation was not carried out, because the results obtained there were characterized by similar values to the results obtained in the Krakow waste incineration plant. To assess whether there is a statistically significant difference between the results obtained in Hinwil and Krakow waste incineration plants, one sample t-test was performed. The test was carried out in two variants, checking whether the mean value of the analyzed data differs from the mean value observed at the Hinwil incinerator, and then one-tailed tests were performed to assess the direction of the change in values.

For silver, the statistic value was 0.75 with a p-value of 0.77. This indicates the acceptance of an alternative hypothesis that the sample average value in the population analyzed in this work differs significantly from the comparable value and is higher than 5,300 ppb.

In the case of gold, the value of the statistic was -0.53 with a p-value of 0.30. In addition, in this case, this indicates the acceptance of an alternative hypothesis that the average value in the population differs from 400 ppb and is lower.

The average platinum content of the analyzed data is also lower than that observed at the Hinwil plant. The value of the statistics was -25.52 with a p-value of 2.2e-16.

When comparing the mean values in the analyzed IBA samples with the mean crustal contents of these elements, it can be seen that they are many times higher in the discussed samples. The silver content in the Earth's crust is 7.5 ppb, gold 0.04 ppb, platinum 0.05, and palladium 1.5 ppb⁴⁶. One Sample t-test confirmed that in the tested incineration bottom ashes samples, the average values of selected elements are statistically significantly higher than in the Earth's crust. The values are $t = 3.13$ with $p\text{-value} = 0.001$ for silver, $t = 1.93$ with $p\text{-value} = 0.03$ for gold, $t = 2.79$ with $p\text{-value} = 0.003$ for palladium, and $t = 7.77$ with $p\text{-value} = 1.68\text{e-}10$ for platinum.

The IRR is the point at which the function of the relationship between the NPV and the discount rate crosses the axis of the discount rate. A project is profitable when its internal rate of return is higher than the cut-off rate, which is the lowest rate of return acceptable to the investor. The economic break-even point for a project to recover precious metals from bottom ash from municipal waste incineration, determined by an internal rate of return, is 4.4%, which is the highest limiting discount rate that can be achieved assuming the project is profitable. Payback time is the length of time it takes to recover the cost of an investment or to reach the break-even point. The payback time for the discussed project is 25 years (Fig. 7).

Discussion

Gold and silver residues come from lost jewelry and burned electronic devices, mainly silver-soldered components or gold-plated contacts, plated tableware, and medicine. Platinum group metals are used as components of control sensors, and measuring equipment, in the production of medical devices, catalysts, industrial refrigerators, automobile candles, as components of high-grade jewelry, and in electronic devices; PGMs are mainly present in integrated circuits. The presence of precious metals in bottom ash from the incineration of municipal waste with EWC codes 19 12 12 and 20 03 01 indicates the presence of these materials in the incinerated municipal waste. The gold and silver contents in the IBA from municipal waste incineration in Krakow are within the range of observed values of these elements in other incinerators. The content of palladium and platinum is lower than the values found in other studies (Table 1). The variability of the precious metals content is poorly correlated. A low content of one element does not mean a low content of the other elements. The diverse sources of elements in bottom ashes lead to the conclusion that the elemental content is influenced by other factors. The appearance of two factors affecting the variability of the content of silver and gold shows the complexity of the phenomenon of analyzing the content of elements and their extraction from residues from municipal waste incineration. Each of the discussed precious metals is stationary over the analyzed period, with no trend or statistically significant seasonality. As a result, it is possible to calculate the minimum recovery of these elements and the minimum plant revenue for current precious metal purchase prices. Despite relatively

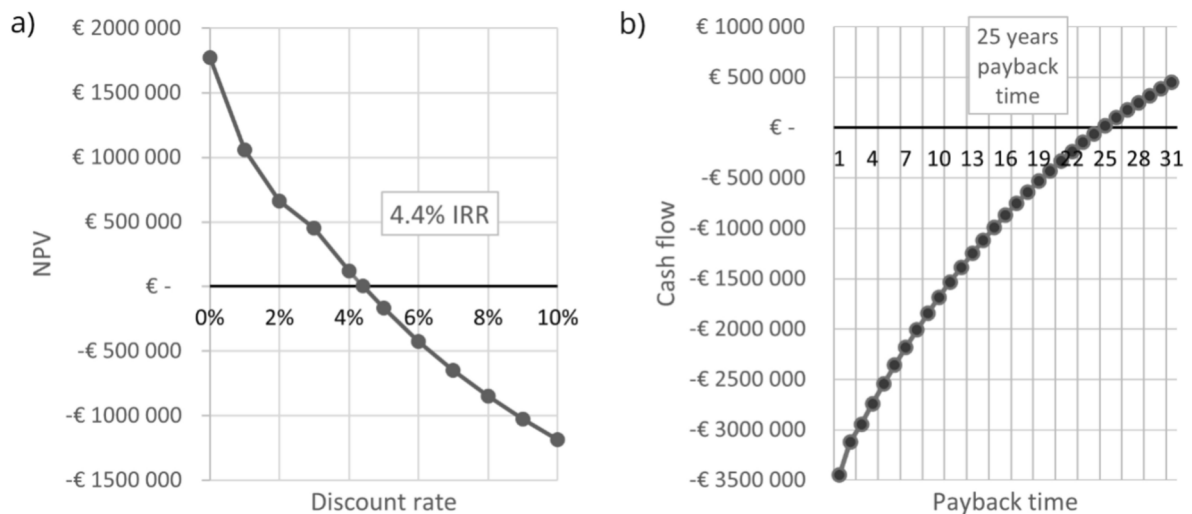


Fig. 7. Investment profitability; (a) internal rate of return for discount rate in the range of 0% to 10%, (b) project payback time.

low average values (median), there are numerous outliers (14–20%) in the case of Ag, Au, and Pt, which can improve the profitability of precious metal recovery, and the use of new separation techniques can lead to an increase in recovery efficiency. The precious metals recovery process uses advanced screening equipment based on a three-stage fractionation method, the so-called Flip flop screens. A characteristic feature of these devices is the use of flexible screens mounted on a transverse structure and the tension and loosening of the screens alternately through the movements of the frame. The material fed to the device is fragmented, then screened in the central area, and intensively fractionated in the last section of the device⁶². The separated <5 mm fine fraction can be directed to a device dedicated to the separation of the heavy metal fraction from the fine fraction of the material using eddy current separation. Separation of the fine-grained bottom ash fraction uses a fine pole system, inducing eddy currents in small IBA fragments with a high frequency of up to 1.3 kHz and a variable pole system rotational speed of up to 4,000 revolutions per minute; the condition for an optimal separation result is to keep the ratio of the upper grain size to the bottom grain size in the bottom ash below an index value of 3⁶³, which is implemented in Hinwil and performs well even in fractions below 1 mm. Further separation of the thus recovered metal concentrate may be carried out using X-ray wave absorption, including X-ray fluorescence and optical separation, the effects of which are achieved through the interaction between high-resolution detectors and multispectral data processing⁶⁴. Very fine fractions below 1 mm as well as finest and randomly distributed oxides fraction may be separated by extraction and chemical leaching, and after which, the metal oxides will be separated⁶⁵. Formation of secondary mineral phases in bottom ash leads to metal binding in two main ways. First, trace amounts of metals are captured in widely distributed minerals that are common in bottom ash. These widely distributed mineral forms, although containing only small amounts of metals, are present in large quantities, leading to significant elemental uptake capabilities. Secondly, minerals that form during the cooling and seasoning processes of bottom ash can capture both trace and larger forms of elements in less widespread minerals. These less prevalent minerals, although less common, may have higher sorption capacities or form more stable compounds with metals. As a result, even small amounts of them contribute significantly to the binding of metals in bottom ash⁶⁶. Random distribution of precious metals may be also controlled by the nugget effect, which is due to the intrinsic properties of the forming materials. It refers to a situation in which there is a large variation in the concentration of precious metals or other components in an IBA sample, caused by the presence of small, highly concentrated structures of the mineral. This effect makes it difficult to accurately determine the average content of constituents in the material under investigation, since small but highly critical element-rich and dispersed bottom ash fragments can significantly affect the results of chemical analysis and ultimately the interpretation of the results. In the context of IBA processing, this means that the intrinsic properties of this waste, lead to a random and irregular distribution of precious metals, which means that their content can vary greatly and the recovery process can be inefficient and difficult to carry out. Despite a number of factors limiting the ability to conduct efficient recovery of precious metals from IBA, their randomness and irregular distribution can improve the overall economic effect of the process^{66,67}. However, the results obtained from the economic evaluation of the project indicate a long payback period for the project. Although the market value of precious metals is high, their amount in IBA and insufficient recovery efficiency of 29–57% make a project focused on the recovery of precious metals unprofitable. By holistically treating the bottom ashes and recovering all possible forms of metals, the economic indicators of the project can be significantly improved. Installations processing bottom ashes are already in operation in most European countries and their average net present value is EUR 84 million. On the contrary, 25% of countries have negative NPV ratios. The average return on this type of installation in Europe is 20% and the highest values above 50% are found in Germany, Spain, Sweden, and the United Kingdom. The average time to reach the break-even point for projects specializing in the recovery of other heavy metal fractions, such as copper, zinc, and light fractions in the form of aluminum

and stainless steel is 11 years, and approximately 67% of projects have a payback time of less than 20 years. The minimum amount of bottom ash for which the economic indicators are positive is 20,000 Mg per year⁵⁵. This means that the planned project may prove to be profitable, provided that a comprehensive approach to the recovery of raw materials from IBA is taken. Therefore, the data preparation, modelling, and evaluation phases in the Cross- Industry Standard Process for Data Mining analysis should be extended to light metal fractions and other heavy metal fractions in bottom ashes from the Thermal Waste Treatment Plant in Kraków.

Conclusions

The silver content in bottom ashes is the highest among all the precious metals and is more than 22 times that of gold, 170 times that of palladium, and more than 525 times that of platinum.

The sum of the precious metals indicates weak and average correlations between their occurrence, which could be seen by the occurrence of both samples with low and high sum values.

Autocorrelation analyzes indicate the stationarity of the elements in the tested IBA samples. However, in the silver autocorrelation plot, one of the lags has a rather high correlation value compared to its neighboring lags. This correlation is not statistically significant. Still, it is worth analyzing the seasonality in the future after the start-up of the precious metal recovery plant to exclude or confirm a change in the nature of the phenomenon.

The box and whisker plots confirmed differences in the amounts of each of the elements during spring, summer, autumn, and winter, but a one-way analysis of variance showed that these were not statistically significant differences.

The relationship between gold and platinum was mostly linear, which is confirmed by the value of Pearson's linear correlation coefficient.

The average values of precious metals in the analyzed samples are many times higher than the values of these elements in the Earth's crust.

The silver content in the Krakow incineration plant was higher than the silver content in the Hinwil installation. The remaining elements were characterized by lower values in the incineration plant.

The economic indicators IRR of 4.4% and payback time of 25 years lead to the conclusion that an installation for the recovery of precious metals is an unprofitable project. The profitability threshold can be met in the case of recovery of other metal fractions from bottom ash, which has been demonstrated in other European installations with a capacity greater than 20,000 Mg per year.

Data availability

The datasets used and analyzed during the current study are available from the corresponding author upon reasonable request.

Received: 5 July 2024; Accepted: 24 February 2025

Published online: 09 March 2025

References

1. Wilson, D. C. & Velis, C. A. Waste management - Still a global challenge in the 21st century: An evidence-based call for action. *Waste Manage. Res.* **33**, 1049–1051 (2015).
2. Eurostat. *Municipal Waste by Waste Management Operations*. Preprint (2023).
3. Gabryszewska, M. & Gworek, B. Impact of municipal and industrial waste incinerators on PCBs content in the environment. *PLOS ONE* **15**, e0242698 (Public Library of Science, 2020).
4. Lam, C. H. K., Ip, A. W. M., Barford, J. P. & McKay, G. Use of incineration MSW ash: A review. *Sustainability* **2**, 1943–1968. Preprint <https://doi.org/10.3390/su2071943> (2010).
5. Godyń, K. & Dutka, B. Preliminary studies of slag and ash from incinerated municipal waste for prospective applications. *Energies (Basel)* **16** (2023).
6. Bauer, G. & Schachermer, E. Statistical analysis of heavy metal data from municipal waste incineration residues. *Environ. Sci. Pollut. Res.* **3**, 10–16 (1996).
7. Council, E. Directive 2008/98/CE of the European Parliament and of the Council of 19 November 2008 on waste and repealing certain Directives. *Off. J. Eur. Union* **L312**, 1–59 (2008).
8. Williams, R., Artola, I., Beznea, A. & Nicholls, G. Emerging challenges of waste management in Europe: Limits of recycling. *Trinomics* (2020).
9. PROGNOS. *Peer Review CEWEP Calculation Tool for Potential Impacts on Waste Amounts for Thermal Treatment*. (2018).
10. Sabbas, T. et al. Management of municipal solid waste incineration residues. *Waste Manag.* **23**, 61–88 (2003).
11. Scarlat, N., Fahl, F. & Dallemand, J. F. Status and opportunities for energy recovery from municipal solid waste in Europe. *Waste Biomass Valoriz.* **10**, 2425–2444 (2019).
12. Shaub, W. M. Municipal solid waste incinerator residues. *Resour. Conserv. Recycl.* [https://doi.org/10.1016/s0921-3449\(97\)00026-8](https://doi.org/10.1016/s0921-3449(97)00026-8) (1997).
13. Al-Ghouti, M. A., Khan, M., Nasser, M. S., Al Saad, K. & Ee Heng, O. O. N. Physiochemical characterization and systematic investigation of metals extraction from fly and bottom ashes produced from municipal solid waste. *PLoS One* **15**, e0239412 (2020).
14. Blasenbauer, D. et al. Legal situation and current practice of waste incineration bottom ash utilisation in Europe. *Waste Manag.* **102**, 868–883 (2020).
15. Wang, X. et al. Removal of heavy metals in municipal solid waste incineration fly ash using lactic acid fermentation broth. *Environ. Sci. Pollut. Res.* **28**, 62716–62725 (2021).
16. Muchova, L., Bakker, E. & Rem, P. Precious metals in municipal solid waste incineration bottom ash. *Water Air Soil Pollut. Focus* **9**, 107–116 (2009).
17. Šyc, M. et al. Metal recovery from incineration bottom ash: State-of-the-art and recent developments. *J. Hazard Mater.* **393** (2020).
18. Astrup, T. et al. Treatment and reuse of incineration bottom ash. In *Environmental Materials and Waste: Resource Recovery and Pollution Prevention*. 607–645 (Elsevier Inc., 2016). <https://doi.org/10.1016/B978-0-12-803837-6.00024-X>.
19. Morf, L. S. et al. Precious metals and rare earth elements in municipal solid waste – Sources and fate in a Swiss incineration plant. *Waste Manag.* **33**, 634–644 (2013).
20. Bunge, R. *Recovery of Metals from Waste Incinerator Bottom Ash*. (2019).

21. Funari, V., Braga, R., Bokhari, S. N. H., Dinelli, E. & Meisel, T. Solid residues from Italian municipal solid waste incinerators: A source for “critical” raw materials. *Waste Manag.* **45**, 206–216 (2015).
22. Balaram, V. Rare earth elements: A review of applications, occurrence, exploration, analysis, recycling, and environmental impact. *Geosci. Front.* **10**, 1285–1303 (2019).
23. Haynes, W. M. CRC handbook of chemistry and physics 95 edition. *J. Am. Pharmaceut. Assoc.* (1942).
24. European Commission. *Study on the Critical Raw Materials for the EU 2023 Final Report*. (2023). <https://doi.org/10.2873/725585>.
25. Bator, J. & Jędrusiak, R. *Municipal Waste Incinerator Market in Poland Municipal Waste Incinerator Market in Poland*. (2023).
26. Dziedzic, D. & Wrona, K. Logistyczny system gospodarowania odpadami na przykładzie Ekospalarni w Krakowie. In *Krakow Review of Economics and Management/Zeszyty Naukowe Uniwersytetu Ekonomicznego w Krakowie*. 85–103 (2022) <https://doi.org/10.15678/ZNUEK.2021.0994.0405>.
27. Polski Komitet Normalizacyjny. PN-EN 14899 Charakteryzowanie odpadów—Pobieranie próbek materiałów—Struktura przygotowania i zastosowania planu pobierania próbek. (2006).
28. Skutan Stefan, Gloor Rolf, M. L. Wykaz metod—Pobieranie i przygotowanie próbek oraz analiza pozostałości stałych z termicznej obróbki odpadów i produktów powstałych podczas ich przetwarzania. *Stiftung Zentrum Nachhaltige Abfall Ressourcennutzung* (2014).
29. Wirth, R. & Hipp, J. CRISP-DM: Towards a standard process model for data mining. In *Proceedings of the 4th International Conference on the Practical Applications of Knowledge Discovery and Data Mining* (2000).
30. Schröer, C., Kruse, F. & Gómez, J. M. A systematic literature review on applying CRISP-DM process model. *Proc. Comput. Sci.* **181**, 526–534 (2021).
31. Chapman, P. et al. CRISP-DM 1.0: Step-by-step data mining guide. (2000).
32. Schneider, J., Seidel, S., Basalla, M. & vom Brocke, J. Reuse, reduce, support: Design principles for green data mining. *Bus. Inf. Syst. Eng.* **65**, 65–83 (2023).
33. Marshall, G. & Jonker, L. An introduction to descriptive statistics: A review and practical guide. *Radiography* **16**, e1–e7 (2010).
34. Singh, A., Maichle, R. & Lee, S. E. *On the Computation of a 95% Upper Confidence Limit of the Unknown Population Mean Based Upon Data Sets with Below Detection Limit Observations* (U.S. Environmental Protection Agency, 2006).
35. Helsén, D. *Nondetects and Data Analysis: Statistics for Censored Environmental Data* (Wiley-Interscience, 2005).
36. Helsén, D. R. *Statistics for Censored Environmental Data Using Minitab and R*. (Wiley, 2012).
37. *Guidance for Data Quality Assessment: Practical Methods for Data Analysis*. (2000).
38. Dégerine, S. & Lambert-Lacroix, S. Characterization of the partial autocorrelation function of nonstationary time series. *J. Multivar. Anal.* **87**, 46–59 (2003).
39. Ostertagová, E. & Ostertag, O. Methodology and application of oneway ANOVA. *Am. J. Mech. Eng.* **1**, 256–261 (2013).
40. Manuca, R. & Savit, R. Stationarity and nonstationarity in time series analysis. *Physica D* **99**, 134–161 (1996).
41. Hauke, J. & Kossowski, T. Comparison of values of Pearson’s and Spearman’s correlation coefficients on the same sets of data. *Quaest. Geogr.* **30**, 87–93 (2011).
42. Headrick, Todd, C. A note on the relationship between the Pearson product-moment and the Spearman rank-based coefficients of correlation. *Open J. Stat.* **06** (2016).
43. Bagdonavičius, V. & Petkevičius, L. Multiple outlier detection tests for parametric models. *Mathematics* **8** (2020).
44. Mishra, P., Singh, U., Pandey, C. M., Mishra, P. & Pandey, G. Application of student’s t-test, analysis of variance, and covariance. *Ann. Card Anaesth.* **22**, 407–411 (2019).
45. Morf, L. S. et al. Precious metals and rare earth elements in municipal solid waste—Sources and fate in a Swiss incineration plant. *Waste Manag.* **33**, 634–644 (2013).
46. Haynes, W. M. CRC handbook of chemistry and physics 95 edition. *J. Am. Pharmaceut. Assoc.* (1942).
47. Ruhl, L., Vengosh, A., Dwyer, G. S., Hsu-Kim, H. & Deonarine, A. Environmental impacts of the coal ash spill in Kingston, Tennessee: An 18-month survey. *Environ. Sci. Technol.* **44**, 9272–9278 (2010).
48. Hand, D. J., Smyth, P. & Mannila, H. *Principles of Data Mining* (MIT Press, 2001).
49. Flores, J. H. F., Engel, P. M. & Pinto, R. C. Autocorrelation and partial autocorrelation functions to improve neural networks models on univariate time series forecasting. In *The 2012 International Joint Conference on Neural Networks (IJCNN)*. 1–8 (2012). <https://doi.org/10.1109/IJCNN.2012.6252470>.
50. Fuller, W. A. *Introduction to Statistical Time Series*. (Wiley Series in Probability and Statistics, 1995).
51. *Data Quality Assessment: Statistical Methods for Practitioners*. (2006).
52. London Metal Exchange. *LBMA Precious Metal Prices*. (2023).
53. Eurostat. *Producer Prices in Industry, Domestic Market - Monthly Data*. (2023).
54. Mehr, J. et al. The environmental performance of enhanced metal recovery from dry municipal solid waste incineration bottom ash. *Waste Manag.* **119**, 330–341 (2021).
55. Bruno, M. et al. Material flow, economic and environmental assessment of municipal solid waste incineration bottom ash recycling potential in Europe. *J. Clean Prod.* **317** (2021).
56. Statista. *Poland: Wholesale Electricity Prices 2023*. (2023).
57. Good, N., Ceseña, E. A. M. & Mancarella, P. *Business Cases. Energy Positive Neighborhoods and Smart Energy Districts: Methods, Tools, and Experiences from the Field* (Elsevier Ltd, 2017). <https://doi.org/10.1016/B978-0-12-809951-3.00006-5>.
58. Bishop, C. M. *Neural Network for Pattern Recognition*. (Oxford University Press, 1995).
59. Morf, L. S. et al. Precious metals and rare earth elements in municipal solid waste - Sources and fate in a Swiss incineration plant. *Waste Manag.* **33**, 634–644 (2013).
60. Buat-Menard, P. & Chesselet, R. Variable influence of the atmospheric flux on the trace metal chemistry of oceanic suspended matter. *Earth Planet Sci. Lett.* **42**, 399–411 (1979).
61. Sałata, A. & Dąbek, L. Methods of assessment of storm water sediments quality. *E3S Web Conf.* **17**, 13 (2017).
62. IFE Aufbereitungstechnik GmbH. *Flip-flop screen TRISOMAT - IFE Aufbereitungstechnik*. (2023).
63. Steinert GmbH. *Eddy Current Fines*. (2023).
64. IMRO Maschinenbau. *Sensor-Based Separation*. (2023).
65. Itam, Z. et al. Extraction of metal oxides from coal bottom ash by carbon reduction and chemical leaching. *Mater Today Proc.* **17**, 727–735 (2019).
66. Piantone, P., Bodénan, F. & Chatelet-Snidaro, L. Mineralogical study of secondary mineral phases from weathered MSWI bottom ash: Implications for the modelling and trapping of heavy metals. *Appl. Geochem.* **19**, 1891–1904 (2004).
67. Eighmy, T. T. et al. Particle petrogenesis and speciation of elements in MSW incineration bottom ashes. In *Studies in Environmental Science* (eds. Goumans, J. J. J. M., van der Sloot, H. A. & Aalbers, Th. G.). Vol. 60. 111–136 (Elsevier, 1994).

Acknowledgements

This research is sponsored by grants from National Natural Science Foundation of China (No. 42373085), and is also supported by the Strategic Priority Research Program of Chinese Academy of Sciences (Grant No. XDB 40000000); Natural Science Basic Research Program of Shaanxi Province (No. 2023-JC-YB-226); Project Supported by the Foundation for Innovative Research Groups of the National Natural Science Foundation of Chi-

na (No. 42221003). Fund of the State Key Laboratory of Loess and Quaternary Geology Chinese Academy of Sciences (No. SKLLQG 2223); We gratefully acknowledge the helpful and valuable comments provided by the editor and the anonymous reviewers, which greatly could improve the manuscript.

Author contributions

All authors contributed to the study conception and design. Material preparation and data collection were performed by Radosław Jędrusiak. Methodology preparation and analysis were performed by Monika Chuchro. Visualizations were performed by Monika Chuchro and Radosław Jędrusiak. Project administration was managed by Barbara Bielowicz. The first draft of the manuscript was written by all authors. Review and editing were performed by Barbara Bielowicz and Monika Chuchro. All authors read and approved the final manuscript.

Funding

This research project was partly supported by the AGH University of Krakow, Faculty of Geology, Geophysics and Environmental Protection, as a part of a statutory project. Research project partly supported by program “Excellence initiative—research university” for the AGH University. Research project supported by program implementation doctorate financed by Ministry of Science and Higher Education.

Competing interests

The authors declare no competing interests.

Additional information

Supplementary Information The online version contains supplementary material available at <https://doi.org/10.1038/s41598-025-91855-7>.

Correspondence and requests for materials should be addressed to M.C.

Reprints and permissions information is available at www.nature.com/reprints.

Publisher’s note Springer Nature remains neutral with regard to jurisdictional claims in published maps and institutional affiliations.

Open Access This article is licensed under a Creative Commons Attribution-NonCommercial-NoDerivatives 4.0 International License, which permits any non-commercial use, sharing, distribution and reproduction in any medium or format, as long as you give appropriate credit to the original author(s) and the source, provide a link to the Creative Commons licence, and indicate if you modified the licensed material. You do not have permission under this licence to share adapted material derived from this article or parts of it. The images or other third party material in this article are included in the article’s Creative Commons licence, unless indicated otherwise in a credit line to the material. If material is not included in the article’s Creative Commons licence and your intended use is not permitted by statutory regulation or exceeds the permitted use, you will need to obtain permission directly from the copyright holder. To view a copy of this licence, visit <http://creativecommons.org/licenses/by-nc-nd/4.0/>.

© The Author(s) 2025, corrected publication 2025